

## **LETTER**

## Photonics integrated circuits using Al $_{x}$ Ga $_{1-x}$ N based UVC light-emitting diodes, photodetectors and waveguides

To cite this article: Richard Floyd et al 2020 Appl. Phys. Express 13 022003

View the <u>article online</u> for updates and enhancements.

## LETTER

## Photonics integrated circuits using $Al_xGa_{1-x}N$ based UVC light-emitting diodes, photodetectors and waveguides



Richard Floyd on, Kamal Hussain, Abdullah Mamun, Mikhail Gaevski, Grigory Simin, MVS Chandrashekhar, and Asif Khan

Department of Electrical Engineering, University of South Carolina, SC 29208, Columbia, United States of America

\*E-mail: rsfloyd@email.sc.edu

Received November 13, 2019; revised December 3, 2019; accepted December 19, 2019; published online January 8, 2020

We report on a study of UVC photonics integrated circuit consisting of monolithically integrated  $Al_xGa_{1-x}N$  multiple quantum wells based light-emitting diodes, detectors and channel waveguides on sapphire substrates. The waveguide stack consisted of a 1.5  $\mu$ m thick n-Al<sub>0.65</sub>Ga<sub>0.35</sub>N waveguide over an AlN (3.5  $\mu$ m thick) clad layer. Using the integrated devices, we estimated the multi-mode ridge waveguide losses to be 23 cm<sup>-1</sup> at  $\lambda_{emission} \sim 280$  nm. We also measured that approximately 80% of the guided light was confined in the  $n^+$ -Al<sub>0.65</sub>Ga<sub>0.35</sub>N layer, 7% in the underlying AlN cladding and the remaining 13% in the double-side polished sapphire substrate. © 2020 The Japan Society of Applied Physics

hotonics integrated circuits (PICs) operating in the UVC spectral region are of significant interest for applications in solar-blind communications, UV Raman spectroscopy, bio-chemical detection and nonlinear optics. 1-5) Since our first report of Al<sub>x</sub>Ga<sub>1-x</sub>N MQW based UVC LEDs on sapphire substrates, significant progress has been made and they are now commercially available from several companies globally. 6,7) Similarly, UVC light detectors using ultra-wide bandgap (UWBG) Al<sub>x</sub>Ga<sub>1-x</sub>N heterojunctions have also been reported by several research groups including ours.<sup>8–10)</sup> Sapphire, due to its optical transparency for wavelengths longer than 200 nm, is primarily the substrate of choice for UVC emitters and detectors. 11-14) For either device type a high quality AlN buffer layer is incorporated prior to the growth of the device active layers which consist of UWBG Al<sub>x</sub>Ga<sub>1-x</sub>N heterojunctions (x > 0.5). AlN is also transparent at UVC wavelengths thereby making the AlN/sapphire templates an ideal cladding layer for Al<sub>x</sub>Ga<sub>1-x</sub>N based UVC guided wave structures. <sup>18)</sup> Nearly all the reported UVC devices to-date have the emitted or detected light in a direction perpendicular to the epilayer surface. For UVC LEDs with emission wavelengths <280 nm, the emitted light is increasingly TM polarized  $(\text{TE/TM} \sim 50\%/50\% \text{ at } \lambda_{\text{emission}} = 280 \text{ nm}).^{19-21)}$  For these wavelengths, it is more favorable for the emitted light to be guided along the lateral direction parallel to the epi-surface. <sup>22–25)</sup>

However, the study of UVC radiation wave-guiding in UWBG  $Al_xGa_{1-x}N$  heterojunctions over sapphire is difficult. Accurate measurement of the guided-mode reflectivity and waveguide cavity losses requires the fabrication of multiple waveguides with varying lengths and identically cleaved facets.<sup>26)</sup> Due to absence of natural cleavage planes, cleaving facets in AlN/sapphire structures is very challenging. However, it is possible to fabricate cleaved facets after thinning the sapphire substrates. 27,28) But grinding and thinning sapphire substrates is in itself a very difficult task due to the hardness of the material. Thus, in addition to the absence of wave-guiding studies, there are also no reports of PIC fabrication in the UVC spectral region All the estimates and measurements of the optical attenuation of metal organic chemical vapor deposited (MOCVD) AlGaN in this spectral region have primarily focused on normal-incidence for the measurement of the optical transmission fringe contrast. <sup>29,30)</sup> It is often difficult to obtain enough fringe contrast at UVC wavelengths because the typical thickness of the absorbing AlGaN layers is only  $\sim 1-2~\mu m$ , which makes the normal-incidence attenuation coefficient difficult to characterize with spectrophotometry. The difficulty is compounded by the effects of surface scattering and the crossing of refractive index barriers at epilayer interfaces.

Here we report on a new approach to fabricate monolithically integrated LEDs, detectors and waveguides in the UVC spectral region. In this approach the UVC emitterdetector pairs are fabricated using the same epilayer structure which also serves as the waveguide coupling between them. This approach circumvents the need for cleaved facets for UVC waveguiding studies. The schematic of our epilayer structure is shown in Fig. 1. It consists of an MOCVD-grown AlN ( $\sim$ 3.5  $\mu$ m)/basal plane sapphire template with a 1.5  $\mu$ m  $n^+$ -Al<sub>0.65</sub>Ga<sub>0.45</sub>N n-contact/cladding  $(N_{\rm d} \sim 2 \times 10^{18} \, {\rm cm}^{-3})$ . It is followed by 4 pairs of  $Al_{0.6}Ga_{0.4}N/Al_{0.35}Ga_{0.65}N$  multiple quantum wells ( $\lambda_{emission}$  $\sim$  280 nm) and an electron blocking AlGaN, a polarization doped graded composition p-AlGaN, and a Mg-doped holeinjection p<sup>+</sup>-GaN cap layer. Mesa type emitter and detector device pairs were then fabricated by first accessing the n<sup>+</sup>-Al<sub>0.65</sub>Ga<sub>0.45</sub>N via inductively coupled plasma reactive ion etching (ICPRIE) and then making the *n*-contacts using a Ti (150 Å)/Al (700 Å)/Ti (300 Å)/Au (500 Å) metal stack. A 30 s 950 °C rapid thermal annealing was used to improve the ohmic behavior and reduce the *n*-contact resistivity which was measured to be  $0.77 \Omega$  mm using standard transmission line measurement test patterns. For the p-contact, Ni/Au was deposited followed by a 5 min 450 °C hot-plate annealing.

The emitter and detector devices of our study share a common epilayer structure which also serves as the waveguide. Figure 2(a) shows an integrated module comprising of detector  $(200 \,\mu\text{m} \times 200 \,\mu\text{m})$ and two emitters  $(100 \, \mu \text{m} \times 100 \, \mu \text{m})$  each. As shown these devices are coupled through the n-Al<sub>0.65</sub>Ga<sub>0.35</sub>N waveguide (the ncontact layer for the devices). In Fig. 2(b) we have plotted the emission power and responsivity as a function of wavelength for the individual devices of our integrated module were performed, using a measurement technique similar to that described elsewhere. 32) The detector responsivity peaks at 1 mA W<sup>-1</sup> (at  $\lambda = 250$  nm) and falls approximately by a factor of  $10^3$  by  $\lambda = 280$  nm which is the peak emission wavelength for the LED emitter. Despite their peak response wavelength difference, there is enough of an

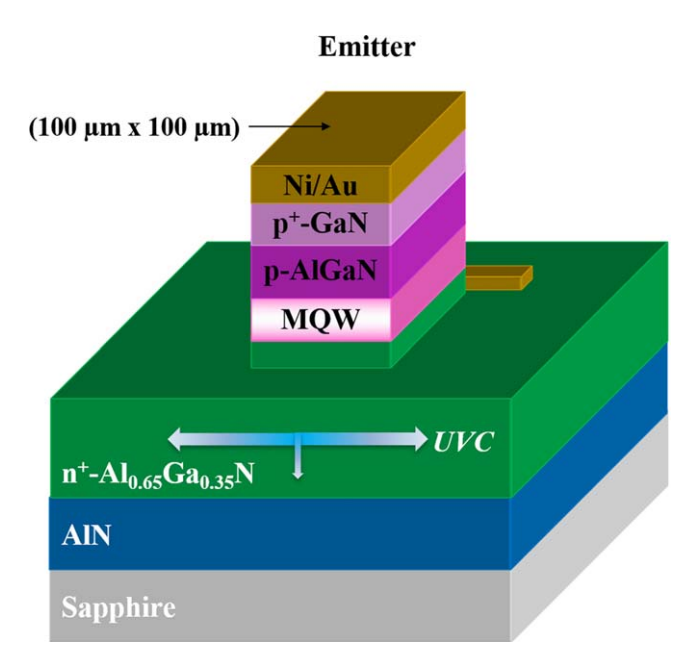


Fig. 1. (Color online) Device epilayer cross section schematic.

overlap in these spectra which gave a strong signal response on the reverse biased detector when either of the emitters were forward biased. This establishes that the same MQW epilayer structure can be employed for the monolithic integration of  $Al_xGa_{1-x}N$  based emitters and detectors for the study of UVC waveguiding and PICs Furthermore, using the capacitance–voltage (C-V) and power–current (L-I)

characteristics of these devices, their total series resistances (emitter = 51  $\,\Omega$ , detector = 33  $\,\Omega$ ) and capacitances (emitter = 50 pF, detector = 44 pF), give an RC time constant of 2.5 ns and 1.2 ns, respectively. This should in principle be capable of supporting a data transfer rate in excess of about 100 Mb s<sup>-1</sup>. 34)

Note our selected device geometry also enables a determination that the detector signal when an emitter is forward biased has no free-space transmission signal. First the emitter 1 of our module was forward biased and the detector signal was measured. Then using a probe tip, UV-absorbing red paint was inserted between them and the signal was measured again. No reduction of the photo-signal confirmed that the detector photo-signal was entirely due to the waveguided UVC radiation from the MQW emitter.

Then, to determine the distribution of guided light among the different layers of our waveguide structure, we measured the detector signal as a function of the depth of a trench that was etched between the adjacent emitter/detector pair of the linear array of Fig. 2(a). For the trench etching which is schematically shown in Fig. 2(c), an ICP-RIE process was used and it resulted in an RMS surface roughness of approximately 2.5 nm. This measured surface roughness was well below the Rayleigh criterion approximation for an optically smooth surface, 350 which conservatively requires RMS roughness <14 nm for specular light transmission. The AlGaN and the AlN layers of our guided-wave structure were completely etched out in steps and after each step the detector photo-signal was recorded. These data are plotted in

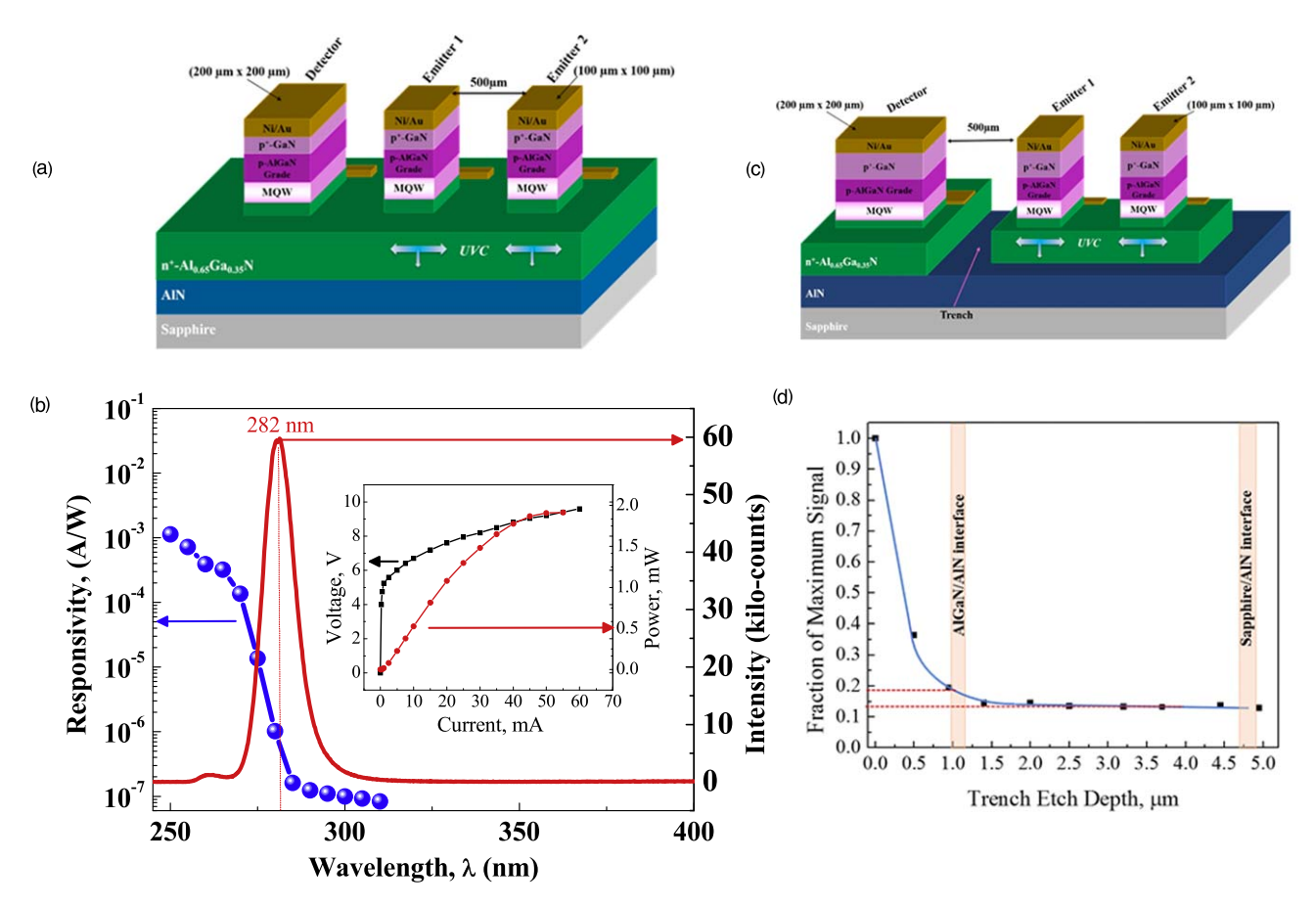


Fig. 2. (Color online) (a) Schematic of linear array of devices. (b) Individual detector and emitter responsivity and emitted power as a function of wavelength. (c) Linear array of devices. Also shown is the etched trench used for power distribution study. (d) Fraction of the waveguided power transmitted between adjacent emitter and detector as a function of the trench depth.

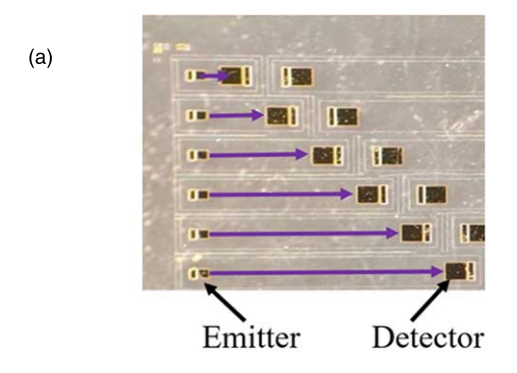
Fig. 2(d). From these data we were able to establish that approximately 80% of the guided light is in the AlGaN waveguide, about 7% in the AlN clad layer and about 13% in the two-sided polished sapphire substrate. Note the uncertainty in these power levels arises from the exact location of the AlGaN/AlN interface and the step-size of the trench etching procedure.

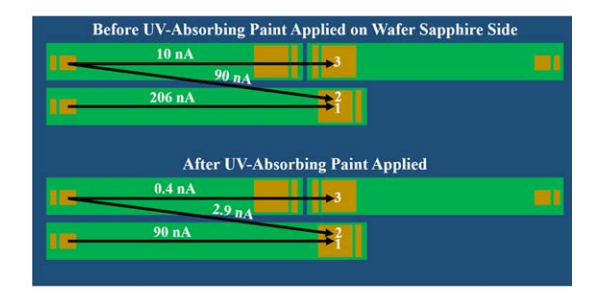
Next, to measure the total waveguide losses, we fabricated the test structure with multiple emitter/detector sets with varying channel waveguide coupling distances between them. The channels were defined using an SiO<sub>2</sub> masking followed by ICPRIE. The channel widths were 340  $\mu$ m. This wide channel geometry was selected to minimize the sidewall scattering losses. The channel etch depth was  $2 \mu m$ . A microscope image of these emitter-detector pairs with varying distances between them is included in Fig. 3(a). We then measured and plotted, in Fig. 3(b), the photocurrent arising from the guided light in the channel waveguide as a function of the detector-emitter spacing. The detector photocurrent was found to increase from the lateral channel confinement due to the air/Al<sub>0.65</sub>Ga<sub>0.35</sub>N ridge sidewall refractive index contrast. We then applied an exponential fit directly to the measured photocurrent versus waveguide length data yielding an attenuation coefficient of 23.35 cm<sup>-1</sup>. Note this number includes both the planar propagation losses and the losses due to sidewall scattering. The use of an optimized fabrication procedures to improve the sidewall roughness in the ICPRIE process is expected to significantly reduce the scattering losses.

We then measured the crosstalk between emitter-detector pairs on adjacent ridges. A top-view schematic of the measurement procedure with the photocurrents overlaid is presented in Fig. 3(c). The crosstalk induced photocurrent arising from the sapphire/AlN transmission is about 45% of the guided-signal strength. This is expected based on our epilayer power distribution measurements of Fig. 2(d). Note, the guided light propagation through the sapphire substrate is nearly double of that through the AlN clad layer. To reduce the crosstalk, the wafer backside was coated with an UV-absorbing paint. This reduced the crosstalk reduced by a factor of 30 while the photocurrent also decreased but only by a factor of 2. This crosstalk is similar to what was reported recently for GaN PICs operating at visible wavelengths. 36)

In summary, we have for the first time demonstrated an UVC PIC using MOCVD-grown monolithically integrated detectors and emitters ( $\lambda_{\rm emission} \sim 280\,\rm nm$ ) and an  $n\text{-Al}_{0.65}\mathrm{Ga}_{0.35}\mathrm{N}$  channel waveguide. The measured attenuation coefficient for multi-mode UVC propagation in this ridge waveguide structure was approximately  $23\,\mathrm{cm}^{-1}$  which establishes the feasibility of using this system for other integrated optical devices and circuits. The fraction of the guided light was estimated to be 80% in the Al $_{0.65}\mathrm{Ga}_{0.35}\mathrm{N}$  layer, 7% in the underlying AlN template and approximately 13% in the sapphire substrate.

Acknowledgments This research was supported by ARO contract W911NF-18-1-0029 monitored by Dr. M. Gerhold. Part of the AlN template work was supported by ONR MURI program monitored by Dr. Lynn Petersen and the DARPA DREAM contract (ONR N00014-18-1-2033), Program Manager Dr. Young-Kai Chen, monitored by Dr. Paul Maki at ONR. The sensor work was partially supported the National Science Foundation (NSF), ECCS Award Nos. 1711322 and 1810116, program director Dr. Dimitris Pavlidis. The authors also





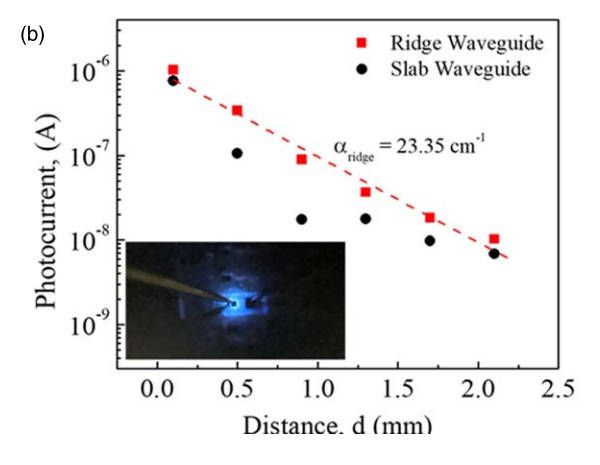


Fig. 3. (Color online) (a) SEM micrograph of devices layout for channel waveguide attenuation measurements. (b) Comparison of slab- and ridge waveguide photocurrents as a function of distance at 10 mA pump current. Inset shows a device under test. (c) Top-view schematic representation of crosstalk measurements performed. We include the photocurrents for each of the measurements with and without a UV-absorbing paint on the wafers sapphire side.

(c)

acknowledge the support from the University of South Carolina through the ASPIRE program.

ORCID iDs Richard Floyd (1) https://orcid.org/0000-0002-1073-9277

- T. J. Lu, M. Fanto, H. Choi, P. Thomas, J. Steidle, S. Mouradian, and J. Kim, "Aluminum nitride integrated photonics platform for the ultraviolet to visible spectrum," Opt. Express 26, 11147 (2018).
- R. Krischek, W. Wieczorek, A. Ozawa, N. Kiesel, P. Michelberger, T. Udem, and H. Weinfurter, "Ultraviolet enhancement cavity for ultrafast nonlinear optics and high-rate multiphoton entanglement experiments," Nat. Photonics 4, 170 (2010).
- B. Mitra, W. Chester, Q. Long, and Y. B. Gianchandani, "A microfluidic ultra-violet emission source for direct fluorescence of tryptophan," Proc. 25th Annual Int. Conf. of the IEEE Engineering in Medicine and Biology Society (IEEE Cat. No. 03CH37439), 2003 (Piscataway, NJ), (IEEE) Vol. 4, pp. 3380–3.
- 4) W. H. P. Pernice, C. Xiong, C. Schuck, and H. X. Tang, "Second harmonic generation in phase matched aluminum nitride waveguides and micro-ring resonators," Appl. Phys. Lett. 100, 223501 (2012).
- H. Jung, R. Stoll, X. Guo, D. Fischer, and H. X. Tang, "Green, red, and IR frequency comb line generation from single IR pump in AlN microring resonator," Optica 1, 396 (2014).
- 6) V. Adivarahan, J. Zhang, A. Chitnis, W. Shuai, J. Sun, R. Pachipulusu, M. Shatalov, and M. A. Khan, "Sub-milliwatt power III-N light emitting diodes at 285 nm," Jpn. J. Appl. Phys. 41, L435 (2002).
- O. Stroh-Vasenev, "More powerful than ever: new chip technology opens new industrial applications for UVC LEDs," Optik Photonik 13, 52 (2018).
- S. Muhtadi, S. M. Hwang, A. L. Coleman, A. Lunev, F. Asif, V. S. N. Chava, M. V. S. Chandrashekhar, and A. Khan, "High-speed solar-blind UV photodetectors using high-Al content Alo. 64Gao. 36N/Alo. 34Gao. 66N multiple quantum wells," Appl. Phys. Express 10, 011004 (2016).
- C. Pernot, A. Hirano, M. Iwaya, T. Detchprohm, H. Amano, and I. Akasaki, "Solar-blind UV photodetectors based on GaN/AlGaN pin photodiodes," Jpn. J. Appl. Phys. 39, L387 (2000).
- 10) R. McClintock, A. Yasan, K. Mayes, D. Shiell, S. R. Darvish, P. Kung, and M. Razeghi, "High quantum efficiency AlGaN solar-blind pin photodiodes," Appl. Phys. Lett. 84, 1248 (2004).
- A. Khan, K. Balakrishnan, and T. Katona, "Ultraviolet light-emitting diodes based on group three nitrides," Nat. Photonics 2, 77 (2008).
- 12) M. Khizar, Z. Y. Fan, K. H. Kim, J. Y. Lin, and H. X. Jiang, "Nitride deepultraviolet light-emitting diodes with microlens array," Appl. Phys. Lett. 86, 173504 (2005).
- 13) P. Dong et al., "282-nm AlGaN-based deep ultraviolet light-emitting diodes with improved performance on nano-patterned sapphire substrates," Appl. Phys. Lett. 102, 241113 (2013).
- 14) Y. Nagasawa and A. Hirano, "A review of AlGaN-based deep-ultraviolet light-emitting diodes on sapphire," Appl. Sci. 8, 1264 (2018).
- 15) J. P. Zhang, H. M. Wang, W. H. Sun, V. Adivarahan, S. Wu, A. Chitnis, and C. Q. Chen et al., "High-quality AlGaN layers over pulsed atomic-layer epitaxially grown AlN templates for deep ultraviolet light-emitting diodes," J. Electron. Mater. 32, 364 (2003).
- 16) M. Imura, K. Nakano, T. Kitano, N. Fujimoto, G. Narita, N. Okada, and K. Balakrishnan et al., "Microstructure of epitaxial lateral overgrown AlN on trench-patterned AlN template by high-temperature metal-organic vapor phase epitaxy," Appl. Phys. Lett. 89, 221901 (2006).
- 17) H. Hirayama, S. Fujikawa, N. Noguchi, J. Norimatsu, T. Takano, K. Tsubaki, and N. Kamata, "222–282 nm AlGaN and InAlGaN-based deep-UV LEDs fabricated on high-quality AlN on sapphire," Phys. Status Solidi A 206, 1176 (2009).
- 18) M. Soltani, R. Soref, T. Palacios, and D. Englund, "AlGaN/AlN integrated photonics platform for the ultraviolet and visible spectral range," Opt. Express 24, 25415 (2016).

- 19) J. E. Northrup, C. L. Chua, Z. Yang, T. Wunderer, M. Kneissl, N. M. Johnson, and T. Kolbe, "Effect of strain and barrier composition on the polarization of light emission from AlGaN/AlN quantum wells," Appl. Phys. Lett. 100, 021101 (2012).
- A. Atsushi Yamaguchi, "Valence band engineering for remarkable enhancement of surface emission in AlGaN deep-ultraviolet light emitting diodes," Physica Status Solidi C 5, pp. 2364 (2008).
- 21) R. G. Banal, M. Funato, and Y. Kawakami, "Optical anisotropy in [0001]oriented Al<sub>x</sub>Ga<sub>1-x</sub> N/AlN quantum wells (x > 0.69)," Phys. Rev. B 79, 121308 (2009).
- 22) J. W. Lee, D. Y. Kim, J. H. Park, E. F. Schubert, J. Kim, J. Lee, Y.-I. Kim, Y. Park, and J. K. Kim, "An elegant route to overcome fundamentally-limited light extraction in AlGaN deep-ultraviolet light-emitting diodes: preferential outcoupling of strong in-plane emission," Sci. Rep. 6, 22537 (2016)
- 23) M. Djavid and Z. Mi, "Enhancing the light extraction efficiency of AlGaN deep ultraviolet light emitting diodes by using nanowire structures," Appl. Phys. Lett. 108, 051102 (2016).
- 24) K. B. Nam, J. Li, M. L. Nakarmi, J. Y. Lin, and H. X. Jiang, "Unique optical properties of AlGaN alloys and related ultraviolet emitters," Appl. Phys. Lett. 84, 5264 (2004).
- 25) Y. Ooi, C. Kee, Liu, and J. Zhang, "Analysis of polarization-dependent light extraction and effect of passivation layer for 230-nm AlGaN nanowire lightemitting diodes," IEEE Photonics J. 9, 1 (2017).
- 26) R. A. Logan and K. R. Franz, "Optical waveguides in GaAs–AlGaAs epitaxial layers," J. Appl. Phys. 44, 4172 (1973).
- 27) Y. Zhang, L. McKnight, E. Engin, I. M. Watson, M. J. Cryan, E. Gu, M. G. Thompson, S. Calvez, J. L. O'Brien, and M. D. Dawson, "GaN directional couplers for integrated quantum photonics," Appl. Phys. Lett. 99, 161119 (2011).
- 28) A. C. Abare, M. P. Mack, M. Hansen, R. K. Sink, P. Kozodoy, S. Keller, and J. S. Speck et al., "Cleaved and etched facet nitride laser diodes," IEEE J. Sel. Top. Quantum Electron. 4, 505 (1998).
- 29) J. F. Muth, J. D. Brown, M. A. L. Johnson, Z. Yu, R. M. Kolbas, J. W. Cook, and J. F. Schetzina, "Absorption coefficient and refractive index of GaN, AlN and AlGaN alloys," Mater. Res. Soc. Internet J. Nitride Semicond. Res. 4, 502 (1999).
- O. Ambacher, R. Dimitrov, D. Lentz, T. Metzger, W. Rieger, and M. Stutzmann, "Growth of GaNAIN and AlGaN by MOCVD using triethylgallium and tritertiarybutylaluminium," J. Cryst. Growth 170, 335 (1997).
- 31) E. Kapon and R. Bhat, "Low-loss single-mode GaAs/AlGaAs optical waveguides grown by organometallic vapor phase epitaxy," Appl. Phys. Lett. 50.23, 1628 (1987).
- 32) V. S. Chava, B. G. Barker Jr., A. Balachandran, A. Khan, G. Simin, A. B. Greytak, and M. V. S. Chandrashekhar, "High detectivity visible-blind SiF4 grown epitaxial graphene/SiC Schottky contact bipolar phototransistor," Appl. Phys. Lett. 111, 243504 (2017).
- 33) M. Shatalov et al., "Lateral current crowding in deep UV light emitting diodes over sapphire substrates," Jpn. J. Appl. Phys. 41, 5083 (2002).
- 34) K. H. Li, W. Y. Fu, Y. F. Cheung, K. K. Y. Wong, Y. Wang, K. M. Lau, and H. W. Choi., "Monolithically integrated InGaN/GaN light-emitting diodes, photodetectors, and waveguides on Si substrate," Optica 5, 564 (2018).
- 35) D. Alden et al., "Fabrication and structural properties of AlN submicron periodic lateral polar structures and waveguides for UV-C applications," Appl. Phys. Lett. 108, 261106 (2016).
- 36) K. H. Li, Y. F. Cheung, W. Y. Fu, K. K. Y. Wong, and H. W. Choi, "Monolithic integration of GaN-on-sapphire light-emitting diodes, photodetectors, and waveguides," IEEE J. Sel. Top. Quantum Electron. 24, 1 (2018).